Letter

New isotope ^{231}Am

J. Khuyagbaatar,[1,*] P. Mosat,[1] J. Ballof,[1] R. A. Cantemir,[1] Ch. E. Düllmann,[1,2,3] K. Hermainski,[1,3] B. Kindler,[1] J. Krier,[1] N. Kurz,[1] S. Löchner,[1] B. Lommel,[1] B. Schausten,[1] P. Wieczorek,[1] and A. Yakushev[1]

[1]*GSI Helmholtzzentrum für Schwerionenforschung GmbH, Darmstadt 64291, Germany*
[2]*Helmholtz Institute Mainz, Mainz 55099, Germany*
[3]*Department Chemie - Standort TRIGA, Johannes Gutenberg-Universität Mainz, Mainz 55099, Germany*

(Received 12 March 2026; accepted 16 June 2026; published 15 July 2026)

The present work aimed at the synthesis of the hitherto unknown ^{231}Am and known ^{229}Am isotopes via the $4n$ evaporation channels of the fusion reactions of ^{48}Ca + ^{187}Re and ^{48}Ca + ^{185}Re, respectively. The new isotope ^{231}Am, with a half-life of 47^{+85}_{-19} s, was identified on the basis of five observed α-decay chains. It emits α particles with an energy of 7.11(2) MeV. An upper limit of 0.66 was estimated for the electron-capture decay branch of ^{231}Am. No α-decay chain from ^{229}Am was observed, corresponding to a cross-section level of 0.03 nb for the detection of a single event. The α-decay properties of ^{231}Am are discussed in the framework of the Geiger-Nuttall empirical relation.

DOI: 10.1103/2clj-zh3s

The study of heavy nuclei far from the β-stability line provides critical insight into nuclear structure and decay properties, particularly in regions where the numbers of protons (Z) and neutrons (N) and their ratio reach extreme values that push the limits of nuclear stability [1–3].

Neutron-deficient actinides near the neutron number $N = 126$ are of particular interest, as they allow investigations of nuclear shell evolution and its effect on their radioactive decay modes such as α, electron capture (EC), and spontaneous fission decays. In the last decade, significant progress has been achieved in the synthesis of U ($Z = 92$) and Np ($Z = 93$) isotopes along $N = 126$, thanks to advanced fast digital electronics that allows measurements of very short-lived nuclei [4–9].

Meanwhile, the production rates of such exotic nuclei in neutron-evaporation channels of the complete fusion reactions decrease rapidly as a function of the compound nucleus' Z [10–12]. Such a strong reduction in production cross section, reaching the level of $\leqslant 0.1$ nb, is typically explained as an effect of a low fission barrier, which reduces both the fusion probability of the reactants and the survival probability of the compound nucleus [10,13–15]. Consequently, the further exploration of nuclei near $N = 126$ towards heavier elements, such as Pu and Am via fusion-evaporation reactions, faces significant production challenges [12]. In this regard, the recently discovered isotope ^{227}Pu contains 133 neutrons [16,17], which is still far from the closed shell at $N = 126$.

In contrast, multinucleon-transfer reactions, which proceed without forming a completely fused compound nucleus, have been shown to be an effective alternative approach for exploring this region. Five very neutron-deficient isotopes ^{216}U, ^{219}Np, ^{223}Am, ^{229}Am, and ^{233}Bk have been synthesized in such multinucleon-transfer reactions [18].

The isotopes ^{223}Am ($N = 128$) and ^{229}Am ($N = 134$) were identified by their α decays, indicating a sudden change in properties compared to heavier Am isotopes (^{230}Am – ^{240}Am), where EC decay dominates.

The competition between the α and EC decay is also of particular interest in Am isotopes, as the latter are the source for studying the EC-delayed fission (ECDF) process [19,20]. Currently, ECDF data for Am, Bk, and Es isotopes constitute the most systematically available experimental data set. This serves as the primary basis for theoretical descriptions of the ECDF process [21–23]. In particular, the exceptionally large ECDF probability measured in ^{230}Am [24] motivates further study of ECDF in more neutron-deficient Am isotopes, such as the hitherto unknown ^{228}Am [23] provided it decays at least partially by EC.

In this regard, systematic studies of the known α-decay properties in the neutron-deficient Am isotopes would be highly valuable. However, such systematics can currently only be established, at most, for the even-N Am isotopes, but even then this systematics remains incomplete as one of the key even-N Am isotopes, namely ^{231}Am, is still unknown.

In this Letter, we report the discovery of the new isotope ^{231}Am in the ^{48}Ca + ^{187}Re fusion-evaporation reaction. These experimental data fill a gap in the systematics of Am isotopes and provide new insights into the evolution of their decay modes.

The experiment was carried out at GSI Helmholtzzentrum für Schwerionenforschung GmbH, Darmstadt, Germany. A pulsed (5 ms long pulses with 50 Hz repetition rate) ^{48}Ca^{10+} beam was accelerated by the Universal Linear Accelerator

*Contact author: J.Khuyagbaatar@gsi.de

UNILAC and irradiated a ^{nat}Re target with an average thickness of about 0.7 mg/cm^2. The four Re-target segments with the isotopic composition of ^{185}Re (37.4%) and ^{187}Re (62.6%) were mounted on a wheel, which rotates synchronously with the beam macrostructure [25]. Two beam energies resulting in center-of-target energies of $E_\mathrm{b} = 220.4$ and 216.8 MeV were used. At these energies the 4n evaporation channels were expected to occur from the ^{233}Am* and ^{235}Am* compound nuclei according to the statistical code HIVAP [26] for fusion-evaporation reactions.

For separation and collection of evaporation residues (ERs) in the focal plane detector (FPD), the Transactinide Separator and Chemistry Apparatus (TASCA) was operated with helium gas at 0.8 mbar pressure and with a magnetic rigidity ($B\rho$) of 1.95 Tm [27,28]. The efficiency of TASCA to guide ERs to the focal plane of TASCA was estimated as 60% [27–29].

The present experiment was performed as part of the commissioning of an ongoing upgrade of the TASCA focal plane detection system. The previous FPD [30], which has been successfully applied at TASCA for nearly two decades, has now been replaced by a 300 μm thick BB20 detector from Micron Semiconductor Ltd. The BB20 recently implemented at the Mass Analyzing Recoil Apparatus (MARA) separator at the University of Jyvaskyla, Finland [31] has been shown to be well suited for radioactive decay studies of the fusion-evaporation products [32,33]. This double-sided silicon strip detector has dimensions of ≈128 mm (horizontal) and ≈48 mm (vertical). The junction-side comprises 192 vertical (X) strips and was facing the separator, while the Ohmic-side has 72 horizontal strips, which provide the (Y) position. In total, 264 signals from the X and Y strips were processed by using 17 charge integrating Mesytec MPRT-16 preamplifiers. Two different preamplifier gains resulting in measured energy ranges up to about 14 and 200 MeV for the X and Y strips, respectively, were used. All preamplified signals were digitized by GSI made FEBEX analog-to-digital converters [35,36]. The shape of each signal was stored in 8000 samples with a sampling frequency of 50 MHz resulting in a trace length of 160 μs. The pretrigger time was 20 μs, which reduces the effective time coverage to 140 μs. This relatively long time enables a safe detection of short-lived α-decaying nuclei above the $N = 126$ shell closure. The rise times of preamplified signals were ≈50 ns. The FPD was operated at room temperature. Amplitudes of the signals were extracted using trapezoidal filters with different parameters, depending on the characteristics of the stored traces [34,37,38]. Figures 1(a) and 1(b) show the summed energy spectra of the 192 X and 72 Y strips, respectively, from the calibration reaction of ^{48}Ca + ^{174}Yb, obtained using two different filters. For the α particles from ^{214}Ra (7.137(3) MeV [39]), best energy resolutions of $\sigma = 14$ and 38 keV were achieved for the X and Y strips, respectively. These values were obtained when the signal amplitude was determined as the average of four samples from a trapezoidal filter with a base and a flat top of 700 and 500 samples, respectively, as indicated in the insets of Fig. 1. For pile-up events with time differences shorter than about 120 samples (i.e., 2.4 μs), amplitudes were extracted using a trapezoidal filter with a base and a flat-top of 30 and 10 samples, respectively (see Fig. 1). The corresponding

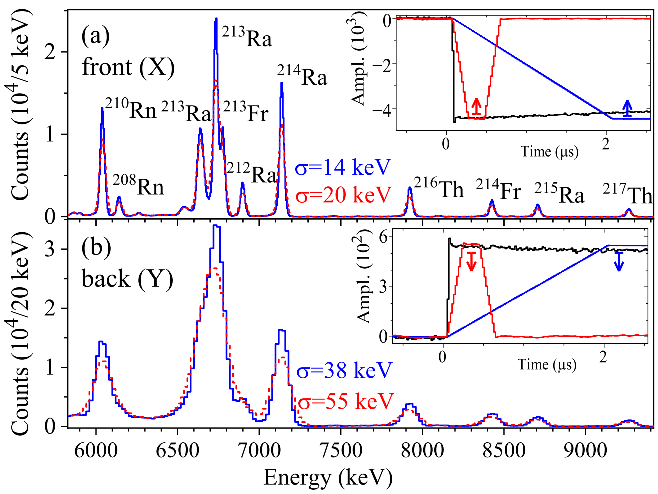

FIG. 1. Summed energy spectra of beam-off events measured in 192 X (a) and 72 Y (b) strips from the ^{48}Ca + ^{174}Yb reaction. The calibrated energies based on signal-amplitudes extracted from two different trapezoidal filters are shown. Insets show the shapes of 7 MeV signals and their shapes after two different trapezoid filters (one with a base of 700 and flat top of 500 samples and the other with 30 and 10 samples for base and flat top, respectively [34]. Arrows mark the positions where average amplitudes of four samples were used for the energy calibrations. The energy resolutions (σ) are given for the peak corresponding to the α decay of ^{214}Ra. See text for details.

resolutions for α particles with an energy of 7.137 MeV were $\sigma = 20$ and 55 keV for the X and Y strips, respectively. This filter allowed to resolve energies of pile-ups down to ≈300 ns.

A multiwire proportional counter (MWPC) typically used to discriminate between events passing through TASCA and events originating from the radioactive decays of implanted ERs, was not used. However, to reduce the energies of incoming ERs, which in turn reduces the amplitude saturation of signals in the low-energy branch (X strips) [40], we mounted a 3.5 μm thick Mylar foil in front (≈3 cm) of the stop detector.

The typical beam intensity of about 0.25 particle μA resulted in an average counting rate of 200 Hz in the FPD. This was largely due to events with low-magnetic rigidity detected during the beam-on periods in lower X-strip numbers [41]. About half of the total counting rate was detected in strips $X = 0$–50.

We searched for nonrandom α-decay chains requiring the spatial (in the same X/Y strips) and time correlations between the α-like events. To cover cascades of α decays of the fusion-evaporation products (e.g., ^{231}Am and ^{228}Np), all events with energies of 6.9–20.0 MeV were considered to be α-like events. The search time of up to 10 s was sufficiently long to cover most α-decay chain members. The α-like event rates during the beam-on and beam-off periods were 47 and 0.002 Hz, respectively, which were distributed over all 13 824 pixels. Once, α-α correlations were identified, further detailed event-by-event and trace analyses were made.

We observed four α-decay chains (No. 1–4) at the beam energy of $E_\mathrm{b} = 220.4$ MeV; they are shown in Fig. 2. Two of them have similar properties and their α members were in fine

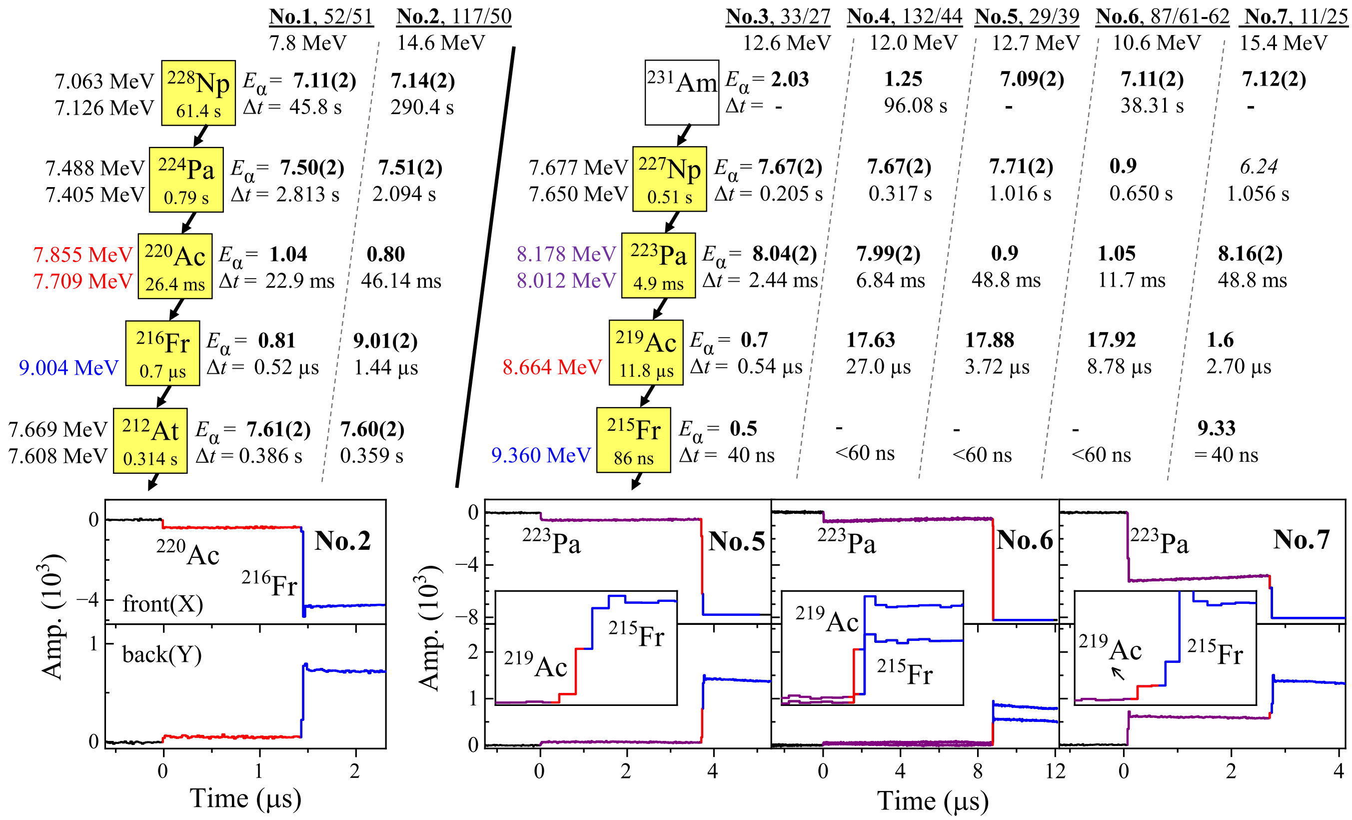

FIG. 2. Upper panels: The properties (α-decay energies and half-lives) of the known members of the ^{228}Np and ^{231}Am decay chains. The observed α-decay chains attributed to originate from these isotopes are shown to the right of the corresponding boxes. Chain number, X and Y strips numbers, and recoil energies are given. Energies of events detected during beam-off periods are given in bold font. Energies are from the X strips except for those of ^{219}Ac (^{215}Fr) in chains (No. 4–7), where full amplitudes were stored only in the traces from Y strips. Lower panels: Representative traces of X and Y strips showing multiple signals corresponding to α decays of short-lived nuclei. Insets show a closer view of the traces (Y strips) in the time regions, where two pile-up α signals with extremely short time differences were detected. See text for details.

agreement with the expected properties of isotopes populated in the α-decay chain originating from ^{228}Np. In both cases, the short-lived ^{216}Fr (0.7 μs) was identified in the trace analyses, i.e., they were found in the traces of the α members assigned to ^{220}Ac. One such trace, measured for the third α member of the chain No. 2, is shown in Fig. 2. One can clearly see that the backward escaped 0.8 MeV α particle of ^{220}Ac was followed by the 9.01(2) MeV α particle of ^{216}Fr after 1.44 μs.

The other two chains (No. 3 and 4) are again similar, but contain α members with properties different from those of the ^{228}Np chain. The properties of these chains fit well to the expected α-decay chain from ^{227}Np, populated by the α decay of the hitherto unknown ^{231}Am. In both chains, however, the first α member, which occurred during the beam-off period, was detected with partial energy corresponding to back-escaped α particles of ^{231}Am. Three more such α-decay chains (No. 5–7), but starting with the same energies [an average of 7.11(2) MeV] of the first α member, were observed when the beam energy was reduced to $E_b = 216.8$ MeV. In all five α-decay chains (No. 3–7), the last two α members were detected in the traces of the α events assigned to ^{223}Pa. Three traces of such events representing the different detection scenarios are shown in Fig. 2. The trace from chain No. 5 shows only two signals corresponding to the escape and pile-up α particles of ^{223}Pa and ^{219}Ac + ^{215}Fr, respectively. The pile-up is due to the very short half-life of 86 ns of ^{215}Fr, which is too short to be fully disentangled into separate signals, given our ≈50 ns rise time and 20 ns of sampling. Another example of traces shown in Fig. 2, for chain No. 6, also consists of a pile-up with signals shared in two neighboring Y strips. In total, three such pile-ups terminated the α-decay chains (No. 4–6), and only an upper limit for the correlation time of 60 ns can be given. The energies of these pile-ups extracted from the Y strips were 17.63, 17.88 and 17.92 MeV, which are in agreement with the sum of the energies of ^{219}Ac and ^{215}Fr (18.024 MeV, see Fig. 2). In two other traces of ^{223}Pa, signals corresponding to α decays of ^{219}Ac and ^{215}Fr could be disentangled and one of them (from chain No. 7) is shown in Fig. 2. A time difference of about 2 samples (40 ns) was observed between the two signals and an energy (Y strip) of the last signal was ≈ 9.33 MeV. Energies and correlation times of members from all chains (No. 3–7) are in agreement with the α-decay properties of ^{227}Np – ^{215}Fr. Based on these results, we attribute all five decay chains to originate from the α decay of the new isotope ^{231}Am.

For all seven chains, we searched for preceding ER-like signals with energies of 7–20 MeV. ER candidates for both chains assigned to ^{228}Np were found and their correlation times are in agreement with the 61.4(1.4) s value measured on the basis of the ECDF of ^{228}Np [39] (see Fig. 2).

In the ^{231}Am chains, ER signals could only be safely assigned for the two chains (No. 4 and 6) observed at higher strip numbers $X = 132$ and 87, where the ER-like event rates are low. A half-life of 47^{+85}_{-19} s was deduced from these two ERs.

We did not detect any α-decay chain originating from ^{231}Pu, which would be produced in the $1p3n$ channel and also in the β/EC decay of ^{231}Am. This gives a lower limit of 0.33 for the α-decay branching of ^{231}Am, estimated by taking the known α-decay branching of ^{231}Pu (≈ 0.1) and five observed α-decay chains of ^{231}Am.

α decay of ^{231}Am with an average α-particle energy of 7.11(2) MeV is attributed as a favored transition between ^{231}Am and ^{227}Np. The deduced Q_α value of 7.24(3) MeV is in agreement with $Q_\alpha = 7.41(31)$ MeV predicted in the atomic mass evaluation for the ground-to-ground state transition. However, due to the large uncertainty of the latter value we do not exclude that the present transition populates an excited state in ^{227}Np.

The present α-decay data for ^{231}Am are compared with the Geiger-Nuttall systematics. In Fig. 3(a), the known experimental data for the most intense, and thus, assumed to be favored α transitions for even-N Am isotopes are shown together with the data for even-N Np, Pu, and Cm isotopes. The even-even Pu and Am isotopes are shown to highlight conservation of a linear dependence between the $\log_{10}(T_\alpha)$ and $Q^{-1/2}$ values, where the effect of electron shell screening was taken into account for Q_α according to Ref. [42]. The experimental data for each element were fit by linear functions by using the well-established α-decay properties. The present experimental data point for ^{231}Am is in good agreement with the expected linear dependency, which was fitted by using the experimental data for $^{233–243}$Am.

On the other hand, noticeable deviation from the linear fit is seen in the case of ^{229}Am. The relatively long half-life of $3.7^{+6.7}_{-1.5}$ s, which we calculated on the basis of two events reported in Ref. [18], cannot be explained by the undetected EC-decay branch, which will only prolong the value shown in Fig. 3. The uncertainty of the experimental Q_α value, which is on the order of 30 keV, should not have a substantial effect and does not lead to the deviations seen in Fig. 3(a). Interestingly, similar deviations are also seen in the cases of ^{228}Pu and ^{225}Np. In fact, it is well established that the linear dependency between the $\log_{10}(T_\alpha)$ and $Q^{-1/2}$ values can be violated when the neutron numbers of nuclei cross the $N = 126$ shell closure [43]. This is likely associated with the formation probability of the α cluster inside the nucleus. In this regard, the enhanced half-lives of the Am and Pu isotopes at $N = 134$ may hint at a similar feature indicating the change in the slope of the linear fit in more neutron-deficient isotopes. If true then one may expect that the hitherto unknown ^{228}Am, which is of particular interest for studying the ECDF, will have a reduced α-cluster formation probability, which may enhance its EC-decay branching. In other words, the α-decay half-life may be longer than 0.1 ms, which is the value predicted by NUBASE2020 [44]. Another possible explanation for the deviations seen in the cases of ^{229}Am and ^{225}Np is

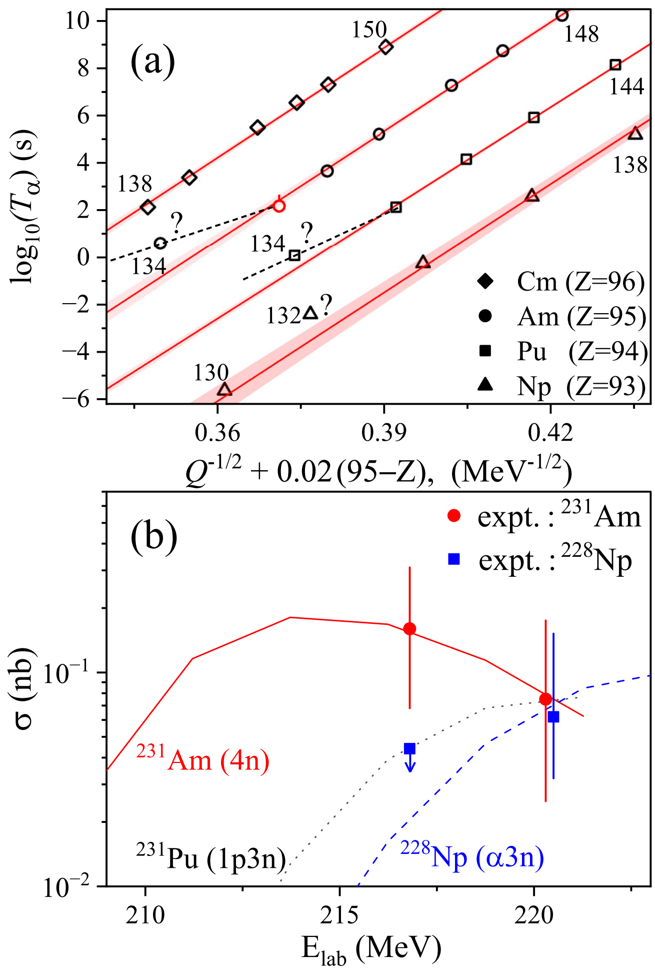

FIG. 3. (a) The Geiger-Nuttall empirical relations shown for the most intense α-decay branches (assumed to be favored transitions) of even-N Np–Am isotopes. The horizontal axis for the particular elements is normalized to $Z = 95$ to avoid the overlapping of data points. Asymmetric errors for the half-lives (e.g., ^{229,231}Am) were derived directly from the absolute upper and lower limits, instead of using the standard error propagation for logarithm functions applied elsewhere. Linear fits of the experimental data marked by solid symbols are shown. The dashed lines are marking the potential violation of the linear dependency. (b) The excitation functions of the $4n$, $1p3n$, and $\alpha3n$ channels from the ^{48}Ca + ^{187}Re reactions according to the HIVAP code are shown by lines together with the presently measured experimental values. See text for details.

that the experimentally observed α decays may not be favored transitions. Nevertheless, these discrepancies motivate further studies of the α-decay properties of these and of the hitherto unknown neutron-deficient Pu and Am isotopes.

The cross sections for the $4n$ and $\alpha3n$ evaporation channels from the ^{48}Ca + ^{187}Re reaction deduced from the measured α-decay chains of ^{231}Am and ^{228}Np are shown in Fig. 3(b). These values are in good agreement with the HIVAP predictions [26], where parameters were used that fit the experimental data of the ^{48}Ca + ^{176}Yb reaction [45]. The simultaneous observation of the $4n$ and $\alpha3n$ channels is common in reactions leading to the formation of neutron-deficient nuclei with $Z > 90$. Such a feature is a signature for the decrease of the fission-barrier heights towards higher Z nuclei.

We did not observe any α-decay chain that may originate from ^{229}Am, which could potentially be produced in the ^{48}Ca + ^{185}Re reaction. Such chains would have been safely identified as the expected chain structure is similar to the ^{231}Am one, i.e., it would consist of three α events stored in the same trace. We estimated the one-event detection sensitivity to be <0.03 and <0.02 nb at $E_b = 220.4$ and 216.8 MeV, respectively, for the 4n channel of the ^{48}Ca + ^{185}Re reaction. Eventually, these levels were not enough to reach a value of 17 pb (at $E_b = 216.8$), which is the maximum cross section predicted by the HIVAP. It is worth noting that ^{229}Am was produced in the multinucleon-transfer reaction ^{48}Ca + ^{248}Cm with a cross section on the order of 5 nb [18], which is more than two orders of magnitude larger than the present one-event limit. In this context, the cross section for the hitherto unknown ^{228}Am in the ^{48}Ca + ^{185}Re was calculated as 1 pb at $E_b = 232$ MeV, which will complicate its ECDF study.

In conclusion, we synthesized the new isotope ^{231}Am in the ^{48}Ca + ^{187}Re reaction and observed its α-decay chains. It decays with an α-particle energy of 7.11(2) MeV and with a half-life of 47^{+85}_{-19} s. We did not observe EC decay of ^{231}Am, which resulted an upper limit of 0.66. In addition, we detected two α-decay chains from ^{228}Np produced as a product of the $\alpha 3n$ channel. The experiment data on ^{231}Am were compared with the α-decay systematics and found to be in good agreement. Experiments on α-decay studies towards more neutron-deficient Am and Pu isotopes are necessary for examining the conservation of the dependency between the half-life and Q value.

Note added. Recently, a parallel study reported the observation of ^{231}Am produced via the α decay of the new isotope ^{235}Bk [46]. The results from [46] are in fine agreement with the present work, where ^{231}Am was produced directly.

We are grateful to GSI's ion-source and UNILAC staff, the Experiment Electronics, and the Target Laboratory departments for their support of the experiment. We acknowledge Dr. I. Rusanov, Dr. S. Minami, and Dr. M. Reese for their support with the fast digital electronics and data acquisition system. We also thank Dr. J. Adamczewski-Musch and Dr. S. Linev for their assistance with the Go4 Analysis Framework, and M. P. Biljan for his assistance in assembling the electronic components. This work was supported by the German BMBF (Grant No. 05P24UM3). The publication is funded by the Open Access Publishing Fund of GSI Helmholtzzentrum für Schwerionenforschung. The results presented here are based on the experiment G-22-00040, which were performed at the beam line X8/TASCA at the GSI Helmholtzzentrum für Schwerionenforschung, Darmstadt (Germany) in the frame of FAIR Phase-0.

Data availability. The data supporting the findings of this study are available within the article.

[1] S. Hofmann and G. Münzenberg, The discovery of the heaviest elements, Rev. Mod. Phys. **72**, 733 (2000).

[2] Yu. Ts. Oganessian, A. Sobiczewski, and G. M. Ter-Akopian, Superheavy nuclei: From predictions to discovery, Phys. Scr. **92**, 023003 (2017).

[3] J. Khuyagbaatar, P. Mosat, J. Ballof, R. A. Cantemir, C. E. Düllmann, K. Hermainski, F. P. Heßberger, E. Jäger, B. Kindler, J. Krier, N. Kurz, S. Löchner, B. Lommel, B. Schausten, Y. Wei, P. Wieczorek, and A. Yakushev, Stepping into the sea of instability: The new sub- μs superheavy nucleus ^{252}Rf, Phys. Rev. Lett. **134**, 022501 (2025).

[4] J. Khuyagbaatar, A. Yakushev, C. E. Düllmann, D. Ackermann, L.-L. Andersson, M. Block, H. Brand, D. M. Cox, J. Even, U. Forsberg, P. Golubev, W. Hartmann, R.-D. Herzberg, F. P. Heßberger, J. Hoffmann, A. Hübner, E. Jäger, J. Jeppsson, B. Kindler, J. V. Kratz, *et al.*, New short-lived isotope ^{221}U and the mass surface near $N = 126$, Phys. Rev. Lett. **115**, 242502 (2015).

[5] M. Sun, Z. Liu, T. Huang, W. Zhang, J. Wang, X. Liu, B. Ding, Z. Gan, L. Ma, H. Yang, Z. Zhang, L. Yu, J. Jiang, K. Wang, Y. Wang, M. Liu, Z. Li, J. Li, X. Wang, H. Lu, *et al.*, New short-lived isotope ^{223}Np and the absence of the $Z = 92$ subshell closure near $N = 126$, Phys. Lett. B **771**, 303 (2017).

[6] H. Yang, L. Ma, Z. Zhang, C. Yang, Z. Gan, M. Zhang, M. Huang, L. Yu, J. Jiang, Y. Tian, Y. Wang, J. Wang, Z. Liu, M. Liu, L. Duan, S. Zhou, Z. Ren, X. Zhou, H. Xu, and G. Xiao, Alpha decay properties of the semi-magic nucleus ^{219}Np, Phys. Lett. B **777**, 212 (2018).

[7] T. H. Huang, W. Q. Zhang, M. D. Sun, Z. Liu, J. G. Wang, X. Y. Liu, B. Ding, Z. G. Gan, L. Ma, H. B. Yang, Z. Y. Zhang, L. Yu, J. Jiang, K. L. Wang, Y. S. Wang, M. L. Liu, Z. H. Li, J. Li, X. Wang, H. Y. Lu, *et al.*, Identification of the new isotope ^{224}Np, Phys. Rev. C **98**, 044302 (2018).

[8] Z. Y. Zhang, Z. G. Gan, H. B. Yang, L. Ma, M. H. Huang, C. L. Yang, M. M. Zhang, Y. L. Tian, Y. S. Wang, M. D. Sun, H. Y. Lu, W. Q. Zhang, H. B. Zhou, X. Wang, C. G. Wu, L. M. Duan, W. X. Huang, Z. Liu, Z. Z. Ren, S. G. Zhou, *et al.*, New isotope ^{220}Np: Probing the robustness of the $N = 126$ shell closure in neptunium, Phys. Rev. Lett. **122**, 192503 (2019).

[9] L. Ma, Z. Y. Zhang, Z. G. Gan, X. H. Zhou, H. B. Yang, M. H. Huang, C. L. Yang, M. M. Zhang, Y. L. Tian, Y. S. Wang, H. B. Zhou, X. T. He, Y. C. Mao, W. Hua, L. M. Duan, W. X. Huang, Z. Liu, X. X. Xu, Z. Z. Ren, S. G. Zhou, and H. S. Xu, Short-lived α -emitting isotope ^{222}Np and the stability of the $N = 126$ magic shell, Phys. Rev. Lett. **125**, 032502 (2020).

[10] K. Jadambaa, The cross sections of fusion-evaporation reactions: The most promising route to superheavy elements beyond $Z = 118$, EPJ Web Conf. **163**, 00030 (2017).

[11] A. Mistry, J. Khuyagbaatar, F. P. Heßberger, D. Ackermann, B. Andel, S. Antalic, M. Block, P. Chhetri, F. Dechery, C. Droese, C. E. Düllmann, F. Giacoppo, J. Hoffmann, O. Kaleja, N. Kurz, M. Laatiaoui, L. Lens, J. Maurer, P. Mosat, J. Piot, *et al.*, The ^{48}Ca + ^{181}Ta reaction: Cross section studies and investigation of neutron-deficient $86 \leqslant Z \leqslant 93$ isotopes, Nucl. Phys. A **987**, 337 (2019).

[12] L. C. Sun, Z. Y. Zhang, Z. G. Gan, S. Y. Xu, M. M. Zhang, J. G. Wang, M. H. Huang, L. Ma, H. B. Yang, H. B. Zhou, N. Wang, C. L. Yang, Y. H. Qiang, X. L. Wu, Y. L. Tian, J. Y. Wang, Y. S. Wang, Z. Zhao, X. Y. Huang, Z. C. Li, *et al.*, Systematics of

production cross sections in ^{54}Cr -induced fusion evaporation reactions, Phys. Rev. C **110**, 014319 (2024).
[13] J. Khuyagbaatar, The superheavy nuclei: Fusion-evaporation reactions, EPJ Web Conf. **306**, 01013 (2024).
[14] D. Vermeulen, H.-G. Clerc, K.-H. Schmidt, J. G. Keller, G. Münzenberg, and W. Reisdorf, Cross sections for evaporation residue production near the $N = 126$ shell closure, Z. Phys. A **318**, 157 (1984).
[15] A. R. Junghans, M. D. Jong, H.-G. Clerc, A. V. Ignatyuk, G. A. Kudyaev, and K.-H. Schmidt, Projectile-fragment yields as a probe for the collective enhancement in the nuclear level density, Nucl. Phys. A **629**, 635 (1998).
[16] H. B. Yang, Z. G. Gan, Z. Y. Zhang, M. H. Huang, L. Ma, C. L. Yang, M. M. Zhang, Y. L. Tian, Y. S. Wang, J. G. Wang, H. B. Zhou, W. Hua, J. Y. Wang, Y. H. Qiang, Z. Zhao, X. Y. Huang, X. J. Wen, Z. Y. Li, H. T. Zhang, S. Y. Xu, *et al.*, α decay of the new isotope ^{227}Pu, Phys. Rev. C **110**, 044302 (2024).
[17] A. A. Kuznetsova, A. I. Svirikhin, A. V. Isaev, M. A. Bychkov, V. D. Danilkin, H. M. Devaraja, N. I. Zamyatin, I. N. Izosimov, Z. Liu, O. N. Malyshev, R. S. Mukhin, A. G. Popeko, Y. A. Popov, V. A. Rachkov, B. Sailaubekov, E. A. Sokol, M. S. Tezekbaeva, I. I. Ulanova, F. Zhang, V. I. Chepigin, *et al.*, Properties of radioactive decay of the new nucleus ^{227}Pu, Phys. Part. Nucl. Lett. **22**, 406 (2025).
[18] H. Devaraja, S. Heinz, O. Beliuskina, V. Comas, S. Hofmann, C. Hornung, G. Münzenberg, K. Nishio, D. Ackermann, Y. Gambhir, M. Gupta, R. Henderson, F. P. Heßberger, J. Khuyagbaatar, B. Kindler, B. Lommel, K. Moody, J. Maurer, R. Mann, A. Popeko, *et al.*, Observation of new neutron-deficient isotopes with $Z \geqslant 92$ in multinucleon transfer reactions, Phys. Lett. B **748**, 199 (2015).
[19] E. Y. Berlovich and Y. N. Novikov, Delayed nuclear fission, Phys. Lett. B **29**, 155 (1969).
[20] A. N. Andreyev, K. Nishio, and K.-H. Schmidt, Nuclear fission: A review of experimental advances and phenomenology, Rep. Prog. Phys. **81**, 016301 (2018).
[21] L. Ghys, A. N. Andreyev, S. Antalic, M. Huyse, and P. Van Duppen, Empirical description of β-delayed fission partial half-lives, Phys. Rev. C **91**, 044314 (2015).
[22] J. Khuyagbaatar, β(EC) delayed fission in the heaviest nuclei, Eur. Phys. J. A **55**, 134 (2019).
[23] J. Khuyagbaatar, R. A. Cantemir, C. E. Düllmann, E. Jäger, B. Kindler, J. Krier, N. Kurz, B. Lommel, B. Schausten, and A. Yakushev, Decay properties of the neutron-deficient isotope ^{242}Es, Phys. Rev. C **109**, 034311 (2024).
[24] G. L. Wilson, M. Takeyama, A. N. Andreyev, B. Andel, S. Antalic, W. N. Catford, L. Ghys, H. Haba, F. P. Heßberger, M. Huang, D. Kaji, Z. Kalaninova, K. Morimoto, K. Morita, M. Murakami, K. Nishio, R. Orlandi, A. G. Smith, K. Tanaka, Y. Wakabayashi, and S. Yamaki, β-delayed fission of ^{230}Am, Phys. Rev. C **96**, 044315 (2017).
[25] E. Jäger, H. Brand, C. E. Düllmann, J. Khuyagbaatar, J. Krier, M. Schädel, T. Torres, and A. Yakushev, High intensity target wheel at TASCA: Target wheel control system and target monitoring, J. Radioanal. Nucl. Chem. **299**, 1073 (2014).
[26] W. Reisdorf, Analysis of fissionability data at high excitation energies, Z. Phys. A **300**, 227 (1981).
[27] J. Khuyagbaatar, D. Ackermann, L.-L. Andersson, J. Ballof, W. Brüchle, C. E. Düllmann, J. Dvorak, K. Eberhardt, J. Even, A. Gorshkov, R. Graeger, F.-P. H. ßberger, D. Hild, R. Hoischen, E. Jäger, B. Kindler, J. Kratz, S. Lahiri, B. Lommel, M. Maiti, *et al.*, Study of the average charge states of ^{188}Pb and ^{252,254}No ions at the gas-filled separator TASCA, Nucl. Instrum. Methods Phys. Res. Sect. A **689**, 40 (2012).
[28] J. Khuyagbaatar, V. P. Shevelko, A. Borschevsky, C. E. Düllmann, I. Y. Tolstikhina, and A. Yakushev, Average charge states of heavy and superheavy ions passing through a rarified gas: Theory and experiment, Phys. Rev. A **88**, 042703 (2013).
[29] K. E. Gregorich, Simulation of recoil trajectories in gas-filled magnetic separators, Nucl. Instrum. Methods Phys. Res. Sect. A **711**, 47 (2013).
[30] A. Gorshkov, A new focal plane detector for the gas-filled separator TASCA, Ph.D. thesis, Technical University of Munich, 2010, https://mediatum.ub.tum.de/node?id=980516.
[31] J. Sarén, J. Uusitalo, and H. Joukainen, In-flight recoil separators RITU and MARA and the standard detector setups, Nucl. Instrum. Methods Phys. Res. Sect. B **541**, 33 (2023).
[32] K. Auranen, A. D. Briscoe, L. S. Ferreira, T. Grahn, P. T. Greenlees, A. Herzáň, A. Illana, D. T. Joss, H. Joukainen, R. Julin, H. Jutila, M. Leino, J. Louko, M. Luoma, E. Maglione, J. Ojala, R. D. Page, J. Pakarinen, P. Rahkila, J. Romero, *et al.*, Nanosecond-scale proton emission from strongly oblate-deformed ^{149}Lu, Phys. Rev. Lett. **128**, 112501 (2022).
[33] A. D. Briscoe, R. D. Page, J. Uusitalo, D. T. Joss, M. A. AlAqeel, B. Alayed, B. Andel, S. Antalic, K. Auranen, H. Ayatollahzadeh, H. Badran, L. Barber, G. Beeton, M. Birova, V. Bogdanoff, R. M. Clark, J. G. Cubiss, D. M. Cullen, J. Deary, U. Forsberg, *et al.*, Decay spectroscopy at the two-proton drip line: Radioactivity of the new nuclides ^{160}Os and ^{156}W, Phys. Lett. B **847**, 138310 (2023).
[34] V. Jordanov *et al.*, Digital techniques for real-time pulse shaping in radiation measurements, Nucl. Instrum. Methods Phys. Res., Sect. A **353**, 261 (1994).
[35] N. Kurz, J. Hoffmann, S. Minami, and W. Ott, The MBS Data Acquisition System for the Search of Element 120 at TASCA, GSI Sci. Rep. **2011**, 252 (2012).
[36] https://www.gsi.de/work/forschung/experimentelektronik.
[37] J. Khuyagbaatar, H. Brand, R. A. Cantemir, C. E. Düllmann, M. Götz, S. Götz, F. P. Heßberger, E. Jäger, B. Kindler, J. Krier, N. Kurz, B. Lommel, B. Schausten, and A. Yakushev, Isomeric states in ^{256}Rf, Phys. Rev. C **103**, 064303 (2021).
[38] J. Khuyagbaatar, R. Cantemir, C. E. Düllmann, F. P. Heßberger, E. Jäger, B. Kindler, J. Krier, N. Kurz, B. Lommel, P. Mosat, B. Schausten, and A. Yakushev, Search for µs-isomers in $^{251-254}$No, Nucl. Phys. A **1070**, 123382 (2026).
[39] NNDC, National Nulcear Data Center, https://www.nndc.bnl.gov/.
[40] J. Khuyagbaatar, A. K. Mistry, D. Ackermann, L.-L. Andersson, M. Block, H. Brand, C. E. Düllmann, J. Even, F. Heßberger, J. Hoffmann, A. Hübner, E. Jäger, B. Kindler, J. Krier, N. Kurz, B. Lommel, B. Schausten, J. Steiner, A. Yakushev, and V. Yakusheva, The identification and confirmation of isomeric states in ^{254}Rf and ^{255}Rf through conversion electron detection, Nucl. Phys. A **994**, 121662 (2020).
[41] J. Khuyagbaatar, A. Yakushev, C. E. Düllmann, D. Ackermann, L.-L. Andersson, M. Asai, M. Block, R. A. Boll, H. Brand, D. M. Cox, M. Dasgupta, X. Derkx, A. Di Nitto, K. Eberhardt, J. Even, M. Evers, C. Fahlander, U. Forsberg, J. M. Gates, N. Gharibyan, *et al.*, Fusion reaction ^{48}Ca + ^{249}Bk leading to formation of the element Ts ($Z = 117$), Phys. Rev. C **99**, 054306 (2019).

[42] J. O. Rasmussen, in *Alpha-, Beta-, and Gamma-Ray Spectroscopy*, edited by K. Siegbahn (North-Holland, Amsterdam, 1966), p. 701.
[43] C. Qi, A. N. Andreyev, M. Huyse, R. J. Liotta, P. Van Duppen, and R. Wyss, On the validity of the Geiger–Nuttall alpha-decay law and its microscopic basis, Phys. Lett. B **734**, 203 (2014).
[44] F. Kondev, M. Wang, W. Huang, S. Naimi, and G. Audi, The NUBASE2020 evaluation of nuclear physics properties, Chin. Phys. C **45**, 030001 (2021).
[45] C.-C. Sahm, H.-G. Clerc, K.-H. Schmidt, W. Reisdorf, P. Armbruster, F. P. Heßberger, J. G. Keller, G. Munzenberg, and D. Vermeulen, Fusion probability of symmetric heavy, nuclear systems determined from evaporation-residue cross sections, Nucl. Phys. A **441**, 316 (1985).
[46] J. Wang, Z. Li, Z. Zhang, Z. Gan, A. Andreyev, M. Huang, L. Ma, M. Zhang, H. Yang, C. Yang, Y. Qiang, Z. Li, X. Huang, G. Xie, L. Zhu, H. Zhou, X. Zhang, J. Zheng, S. Xu, Z. Zhao, *et al.*, Decay properties of new isotopes ^{235}Bk and ^{231}Am, Phys. Lett. B **875**, 140365 (2026).